Inhibition of Carbonic Anhydrase

Kenneth M. Merz, Jr.,*,† Mark A. Murcko,‡ and Peter A. Kollman§

Contribution from the Department of Chemistry and Department of Molecular and Cell Biology, The Pennsylvania State University, University Park, Pennsylvania 16802, Molecular Systems Department, Merck, Sharp and Dohme Research Laboratories, West Point, Pennsylvania 19486, and Department of Pharmaceutical Chemistry, University of California, San Francisco, San Francisco, California 94143. *Received September 15, 1989*

Abstract: We report free energy perturbation simulations on a series of sulfonamide ($RS(O)_2NH^-$) inhibitors of the zinc metalloenzyme human carbonic anhydrase II (HCAII). In order to carry out these simulations, we had to incorporate the zinc ion into the AMBER force field. To do this, we have found that the following modifications are appropriate: (1) the charge on zinc was reduced from +2.0 to +0.8; (2) explicit covalent bonds and angles were incorporated between the zinc and its ligands (His 94, His 96, His 119). This model was determined by parametrizing the force field against the known structure of a HCAII-acetazolamide complex. The series of compounds examined include *p*-hexylbenzenesulfonamide (**1**), benzenesulfonamide (**2**), and *p*-hexylbenzenesulfonate (**3**). Two conversions were studied: the first involved the direct conversion of **1** into **2**, while the second involved changing the sulfonamide group to a sulfonate (**1** → **3**). The former simulation involved direct conversion of a hexyl group into a hydrogen atom, an ambitious calculation, which has provided insight into the capabilities of the free energy perturbation method. We find that we can reproduce experimental relative binding constants but that this ability to do so is very dependent on the molecular mechanical model used and on the simulation protocol. In order for us to compare our calculated results with experimental ones for the latter simulation, we have had to account for the pK_a difference between the sulfonamide and a sulfonate groups. With the appropriate correction for the pK_a difference between **1** and **3** we find that we are able to reproduce the experimental $\Delta\Delta G_{bind}$. We also find that the reason why sulfonamides are better inhibitors of HCAII than are sulfonates can be traced to a single hydrogen-bond interaction present in sulfonamides, but lacking in sulfonates.

Introduction

The human carbonic anhydrases (HCA) are a family of zinc-requiring metalloenzymes that catalyze the interconversion of carbon dioxide and bicarbonate.[1] Seven distinct isozymes have been observed, which can be designated HCAI-HCAVII.[1] Forms I-III have maximal turnover numbers of 1×10^5, 1×10^6, and 1×10^4 at 25 °C, respectively. Drugs that inhibit HCAII are very useful in the treatment of glaucoma,[2,3] which they mitigate by reducing interocular pressure.[3] Since we are focusing on drug design issues as they relate to carbonic anhydrase, we will exclusively focus on inhibition of the HCAII isozyme. Extensive studies on the inhibition of HCAII have demonstrated that the sulfonamides ($RS(O)_2NH^-$) are the most *therapeutically* useful compounds in accomplishing this task.[4]

The mode by which sulfonamides inhibit this enzyme is via the direct ligation of the sulfonamide moiety to the zinc ion.[5] The sulfonamide inhibitor is thought to be bound to the enzyme in its anionic form and not its neutral form.[5] Figure 1 gives a picture of a sulfonamide bound to HCAII. The histidine nitrogen to zinc distance is, on average, 2.08 Å, the sulfonamide nitrogen to zinc bond distance is 2.0 Å, and the sulfonamide oxygen to zinc distance is 3.12 Å. These distances indicate that the coordination sphere is that of a distorted tetrahedron. Note also that HN1 is hydrogen bonded to OG1 of Thr 199 and HOG is hydrogen bonded to OE1 from Glu 106. A final interaction of note is the hydrogen bond between HN from Thr 199 and O2 from the inhibitor. All of these interactions add to the stability of the sulfonamide-HCAII complex and thus enhance the ability of sulfonamides to inhibit the action of HCAII.

Several HCAII-sulfonamide structures have been solved crystallographically[5] and have been recently refined,[6] thereby providing us with a starting point for our thermodynamic cycle-free energy perturbation (TC-FEP) simulations. There is also a large amount of K_i data, covering a wide activity range, on numerous substituted sulfonamides, of which ref 4 only lists a few. In the present study we have chosen the following series of compounds for study: *p*-hexylbenzenesulfonamide (**1**), benzenesulfonamide (**2**), and *p*-hexylbenzenesulfonate (**3**). The reasoning

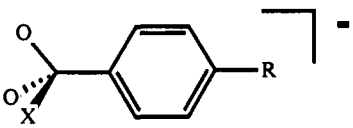

1: X = NH, R = hexyl
2: X = NH, R = H
3: X = O, R = hexyl

for our choices is as follows: One of the most interesting features of the HCAII active site cleft, besides the fact that it is deep (15 Å) and wide (15 Å), is its division into hydrophobic and hydrophilic regions.[1] Thus, it is possible that **1** takes advantage of, by virtue of its alkyl "tail", the hydrophobic portion of the active site, while **2** would to a much lesser extent. The present work will address this issue. Furthermore, a TC-FEP simulation in which a hexyl group is disappearing would provide us with a difficult test case, in which we will be able to simultaneously address sampling issues, simulation protocol issues, and force field accuracy. Also, due to the structural similarity between sulfonates and sulfonamides we wanted to understand why the former are poorer HCAII inhibitors than the latter. Finally, these latter

† The Pennsylvania State University.
‡ Merck, Sharp and Dohme Research Laboratories.
§ University of California, San Francisco.

(1) For some recent reviews, see: Silverman, D. N.; Lindskog, S. *Acc. Chem. Res.* **1988**, *21*, 30. Lindskog, S. In *Zinc Enzymes*; Spiro, T. G., Ed.; Wiley: New York, 1983; p 77. Silverman, D. N.; Vincent, S. H. *CRC Crit. Rev. Biochem.* **1983**, *14*, 207. Lipscomb, W. N. *Annu. Rev. Biochem.* **1983**, *52*, 17. Bertini, I.; Luchinat, C.; Scozzafava, A. *Struct. Bonding (Berlin)* **1981**, *48*, 45. Pocker, Y.; Sarkanen, S. *Enzymol.* **1978**, *47*, 149. For a good description on the family of HCAs see: Tashian, R. E. *Bioessays* **1989**, *10*, 186.

(2) Zimmerman, J. J. *Ann. Ophthalmol.* **1978**, *10*, 509.

(3) Becker, B. *Am. J. Ophthalmol.* **1954**, *37*, 13. Friedenwald, J. C. *Am. J. Ophthalmol.* **1949**, *32*, 9.

(4) See for example: Ponticello, G. S.; Freedman, M. B.; Habecker, C. N.; Lyle, P. A.; Schwam, H.; Varga, S. L.; Christy, M. E.; Randall, W. C.; Baldwin, J. J. *J. Med. Chem.* **1987**, *30*, 591. Kishida, K.; Miwa, Y.; Iwata, C. *Exp. Eye Res.* **1986**, *43*, 981. King, R. W.; Burgen, A. S. V. *Proc. R. Soc. London, B* **1976**, *193*, 107. Mann, T.; Keilin, D. *Nature* **1940**, *146*, 164. Maren, T. H. *Physiol. Rev.* **1967**, *47*, 595. See also refs 1-3.

(5) Kannan, K. K.; Vaara, I.; Nostrand, B.; Lövgren, S.; Borrell, A.; Fridborg, K.; Petef, M. In *The Proceedings on Drug Action at the Molecular Level*; Roberts, G. C. K., Ed.; University Park Press: Baltimore, 1977; p 73.

(6) Eriksson, E. A.; Jones, T. A.; Liljas, A. In *Zinc Enzymes*; Bertini, I., Luchinat, C., Maret, W., Zeppezauer, M., Eds.; Birkhäuser: Boston, 1986; p 317. Eriksson, A. E.; Jones, A. T.; Liljas, A. *Proteins* **1989**, *4*, 274. Eriksson, A. E.; Kylsten, P. M.; Jones, T. A.; Liljas, A. *Proteins* **1989**, *4*, 283.

0002-7863/91/1513-4484$02.50/0

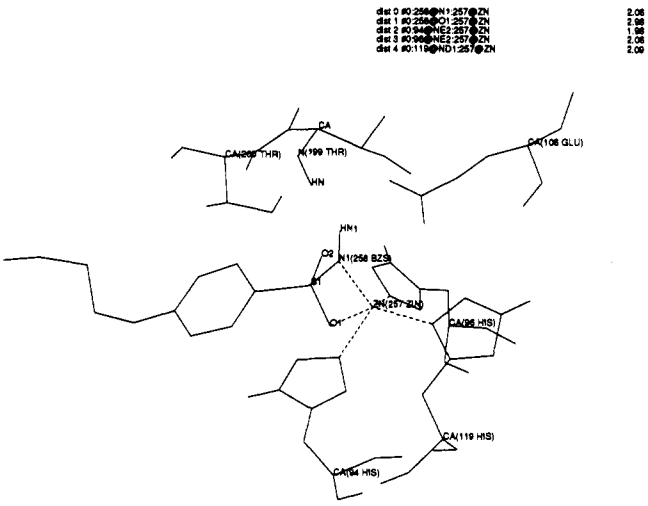

Figure 1. View of the HCAII active site with **1** bound.

simulations pose a problem for the computer simulator because of the differences in the pK_a's of the sulfonamide and sulfonate moieties. Hence, we have had to correct the experimental inhibition constants to remove the pK_a dependence in order to make direct comparisons to our calculated free energies. The combination of the fact that sulfonamides are useful and very specific drugs and the study of these drugs provides useful paradigms for the TC-FEP methodology makes this research of topical interest.

Computational Approach

The free energy perturbation method is a statistical mechanical approach first described by Zwanzig[7] that has recently found extensive application[8] due, in no small part, to the recent advances in computer technology.

The Gibbs free energy can be calculated according to eq 1,[7] where k_B is Boltzmann's constant, T is the absolute temperature, $H(\lambda+\Delta\lambda)$ and $H(\lambda)$ are the Hamiltonians at the states λ and $\lambda + \Delta\lambda$, and the $\langle\rangle_\lambda$ indicates the ensemble average at the intermediate points along the conversion pathway defined by the coupling parameter λ. A molecular

$$\Delta G_l = G(\lambda+\Delta\lambda) - G(\lambda) = -k_B T Ln\langle e^{-(H(\lambda+\Delta\lambda)-H(\lambda)/k_B T)}\rangle_\lambda \quad (1)$$

dynamics (MD) or Monte Carlo simulation is then run between the states $\lambda = 1$ to $\lambda = 0$ (or the reverse) where the free energy is evaluated at each of the intermediate λ points. The total free energy for this change is then given by eq 2 where N is the number of windows or points used to effect the conversion from $\lambda = 1$ to $\lambda = 0$.

$$\Delta G_{total} = \sum_{l=1}^{N} \Delta G_l \quad (2)$$

In order to determine the $\Delta\Delta G_{bind}$ between one inhibitor and another, we make use of the thermodynamic cycle in Scheme I, where ΔG_{inhib} and $\Delta G_{inhib'}$ represent the free energy of binding of the inhibitors S and S', respectively, ΔG_{sol} represents the free energy of solvation difference between S and S', and ΔG_{bind} represents the free energy of binding difference between S and S' in the enzyme active site. Using simulations, we are currently unable to determine the ΔG_{inhib} terms, because of the long time scales and the large perturbations that are necessary to model this process; however, it is possible to mutate one inhibitor into another and thereby readily determine ΔG_{sol} or ΔG_{bind}. Since we are dealing with a state function (ΔG), the relationship (eq 3), based on the thermodynamic cycle, holds. Thus, we have at our disposal all that is necessary to determine the $\Delta\Delta G_{bind}$ between two inhibitors.

$$\Delta\Delta G_{bind} = \Delta G_{inhib'} - \Delta G_{inhib} = \Delta G_{bind} - \Delta G_{sol} \quad (3)$$

Scheme I

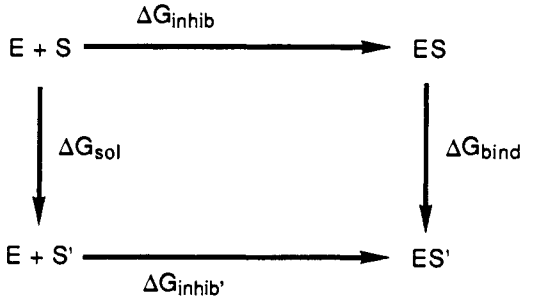

Table I. AMBER Force Field Parameters for the Zinc Ion and Its Ligands

bonded parameter	K_X[a]	X_0
Zn–N	100 kcal/mol·Å^2	2.0 Å
N–Zn–N	50 kcal/mol·rad^2	109.5°
Zn–N–C	10 kcal/mol·rad^2	126.0°
nonbonded parameters	R^* (Å)	ϵ (kcal/mol)
Zn	1.4	0.1

[a] X is R (bond length) or θ (bond angle). X_0 is the reference bond length or angle.

Parametrization. A common procedure for the incorporation of a metal ion into a protein is to assume that the ion carries its full formal charge and that it will retain its observed coordination number and position through a combination of Lennard-Jones and electrostatic interactions.[9] However, we have found that due to the presence of negatively charged residues in the active site of HCAII and the +2 charge of Zn, the zinc ion tends to become hexacoordinated during the course of a MD simulation regardless of our choice of Lennard-Jones parameters. One approach to solving this problem is to restrain specific atoms at their crystallographically observed position. This is the approach that was used in our recent work on thermolysin.[10] However, restraining atoms reduces the conformational flexibility of residues that are sometimes in close proximity to the perturbation site, thereby potentially affecting the computed free energies. Another approach removes the Coulombic term from the force field entirely and relies on the remaining Lennard-Jones like terms of the force field to retain the structural integrity of the system being studied.[11] In light of the obvious importance of electrostatic interactions in proteins and the fact that such an approach would not let us calculate a $\Delta\Delta G_{bind}$ for **1** to **3**, we did not adopt this procedure. Thus, it is desirable to parametrize the charges in our force field such that it will, in a realistic manner, better reproduce the structure of the active site. We used the recently reevaluated HCAII–acetazolamide X-ray structure[6] as a template for our parametrization efforts.

The first important issues we tackled were the following. What is a reasonable charge for the zinc ion, and in what manner might we displace the excess charge on the zinc ion? We used the semiempirical SCF-MO method AM1[12] as implemented by the AMPAC[13] (MOPAC[14]) suite of programs. AM1 has been parametrized for zinc[15] and thus provides us with a useful and fast method by which we might determine the charge of a zinc ion in a similar environment as that contained in the HCAII active site. The results for a number of model calculations on the active site model $(Im)_3ZnX$ ($X = NH_2^-$, OH^-, H_2O, NH_3) suggested that the zinc ion should carry a charge of +0.6. However, we found that the zinc ion, with a charge of approximately +0.6, still had a tendency to form a hexacoordinated structure during the course of a MD simulation. We decided that in order to overcome this we would have to insert explicit bonds (Zn–N) and explicit angles (N–Zn–N and Zn–N–C) between the

(7) Zwanzig, R. W. *J. Chem. Phys.* **1954**, *22*, 1420.

(8) See for example: Potsma, J. P. M.; Berendsen, H. J. C.; Haak, J. R. *Faraday Symp.* **1982**, *17*, 55. Tembe, B. L.; McCammon, J. A. *J. Comput. Chem.* **1984**, *8*, 281. Jorgensen, W. L.; Ravimohan, C. *J. Chem. Phys.* **1985**, *83*, 3050. Bash, P. A.; Singh, U. C.; Langridge, R.; Kollman, P. A. *Science* **1987**, *236*, 564. Singh, U. C.; Brown, F. K.; Bash, P. A.; Kollman, P. A. *J. Am. Chem. Soc.* **1987**, *108*, 1607. Rao, B. G.; Singh, U. C. *J. Am. Chem. Soc.* **1989**, *111*, 3125. Gao, J.; Kuczera, K.; Tidor, B.; Karplus, M. *Science* **1989**, *244*, 1069. For recent reviews on free energy methods, see: Jorgensen, W. L. *Acc. Chem. Res.* **1989**, *22*, 184. van Gunsteren, W. F. *Protein Eng.* **1988**, *2*, 5. Mezei, M.; Beveridge, D. L. *Ann. N. Y. Acad. Sci.* **1986**, *482*, 1.

(9) Vedani, A.; Dunitz, J. D. *J. Am. Chem. Soc.* **1985**, *107*, 7653. Vedani, A.; Huhta, D. W.; Jacober, S. P. *J. Am. Chem. Soc.* **1989**, *111*, 4075. Bash, P. A.; Singh, U. C.; Brown, F. K.; Langridge, R.; Kollman, P. A. *Science* **1987**, *235*, 574. Ahlström, P.; Teleman, O.; Kördel, J.; Forsén, S.; Jösson, B. *Biochemistry* **1989**, *28*, 3205.

(10) Merz, Jr., K. M.; Kollman, P. A. K. *J. Am. Chem. Soc.* **1989**, *111*, 5649 and references cited therein.

(11) Vedani, A.; Dobler, M.; Dunitz, J. D. *J. Comput. Chem.* **1986**, *7*, 701.

(12) Dewar, M. J. S.; Zoebisch, E. G.; Healy, E. F.; Stewart, J. J. P. *J. Am. Chem. Soc.* **1985**, *107*, 3902.

(13) Dewar, M. J. S.; Stewart, J. J. P. *Quantum Chem. Prog. Exchange Bull.* **1986**, *6*, 24, QCPE Program 506.

(14) Stewart, J. J. P. *Quantum Chem. Prog. Exchange Bull.* **1986**, *6*, 91, QCPE Program 455, Version 3.1.

(15) Dewar, M. J. S.; Merz, K. M., Jr. *Organometallics* **1988**, *7*, 522.

zinc ion and its histidine ligands. The parameters used are given in Table I. This approach was successful in reproducing the active site geometry. However, we found from preliminary minimizations and molecular dynamics simulations that a charge of +0.6 gave a low electrostatic interaction between the zinc and the sulfonamide, which resulted in a coordination around the zinc ion that did not match the experimental one. A charge of +0.8 in conjunction with a reduction of the sulfonamide oxygen charge by +0.1 (the resulting excess charge was placed on the sulphur to retain a net +1.0 charge for the whole complex) gave a structure for the zinc–sulfonamide complex that was in good agreement with the experimental one.[6] In order to retain charge neutrality, the excess charge from the zinc ion was dispersed onto the histidines surrounding the zinc ion in the active site. From our model calculations on zinc complexes described above, we found that the all the ring atoms except the NH nitrogen (i.e., the nitrogen not bound to zinc) were more positive by approximately +0.1 in the zinc complex than in imidazole itself. On the basis of these results, we modified the AMBER united-atom[16a] data base accordingly. For example, Figure 2 gives the modified AMBER HIE (histidine N^{ϵ} protonated) residue charges and the united-atom and all-atom charges for **1**–**3**. The HID residue was modified in an analogous manner. The use of these charges and the AMBER united-atom model with ionized side chains gave a system that had a net neutral charge.

Computational Procedure. The charges for the three inhibitors (**1**–**3**) were determined by first doing 6-31G*[17] geometry optimizations on methanesulfonamide ($CH_3S(O)_2NH^-$) and on methanesulfonate ($CH_3SO_3^-$). The SO_3^- and SO_2NH^- moieties were then appended to both a benzene ring and a *p*-hexylbenzene moiety. Subsequently, MNDO[18] geometry optimizations were carried out on these molecules, in which the sulfonamide or the sulfonate 6-31G* geometric variables were held fixed. These structures then had their electrostatic potential derived point charges[19] evaluated with use of the STO-3G*[20] basis set. For **1** and **2** the charge on the nitrogen is around –0.975, the NH hydrogen +0.218, the oxygens –0.47, and the sulfur +0.9. For **3** the sulfur charge is still +0.9, but the oxygen charge has increased to –0.54. These charges were then modified as outlined in Parametrization. In all cases the hydrophobic portions of these molecules, as expected, have atomic charges that are close to zero. Having thus obtained the charges for the three inhibitors, we assembled a force field to describe the inhibitor from standard AMBER parameters.[16]

The free energy perturbation calculations were carried out with use of the GIBBS module of the AMBER[21] suite of programs. We initially used the "window" approach for the determination of the free energy.[8] In the solution-phase simulations we placed the inhibitor in question in a box of approximately 800 TIP3P[22] water molecules generated from a Monte Carlo simulation. We then fully minimized this system ($\epsilon = 1$) in order to remove any bad intermolecular contacts. Following minimization, we then equilibrated for 4 ps at constant pressure (1 atm) and temperature (300 K) using periodic boundary conditions.[23] The perturbations were carried out at constant temperature and pressure over 40 windows with a $\Delta\lambda$ of 0.025, and at each window 250 steps of equilibration (0.002-ps time step) and 150 steps of sampling (0.001-ps time step) were employed. For the all-atom no-shrink case only (see below) we have carried out substantially longer simulations that used 600 and 1000 steps of equilibration and 400 and 1000 steps of sampling, respectively. Thus, the solution simulations covered a total of 32.8, 82, and 164 ps for the all-atom case and only 32.8 for the rest. The nonbonded pair list had a cutoff of 8.0 Å and was updated every 50 time steps. A constant dielectric of 1 was used throughout. In order to assess the degree of hysteresis (i.e., the degree of thermodynamic reversibility) in our calculations, we ran simulations in both the forward ($\lambda = 1$ to $\lambda = 0$) and backward ($\lambda = 0$ to $\lambda = 1$) directions.

We explored two possibilities for the treatment of the C–C bonds in the hexyl group during the course of the simulation. One approach is to allow the bonds to slowly "shrink" during the course of the simulation by the linear introduction of a dummy atom–dummy atom distance (0.4 Å) that is substantially shorter than the starting C–C distance (1.53 Å). Another approach is not to shrink the bonds by keeping the dummy atom–dummy atom distance at 1.53 Å. We have explored the use of the

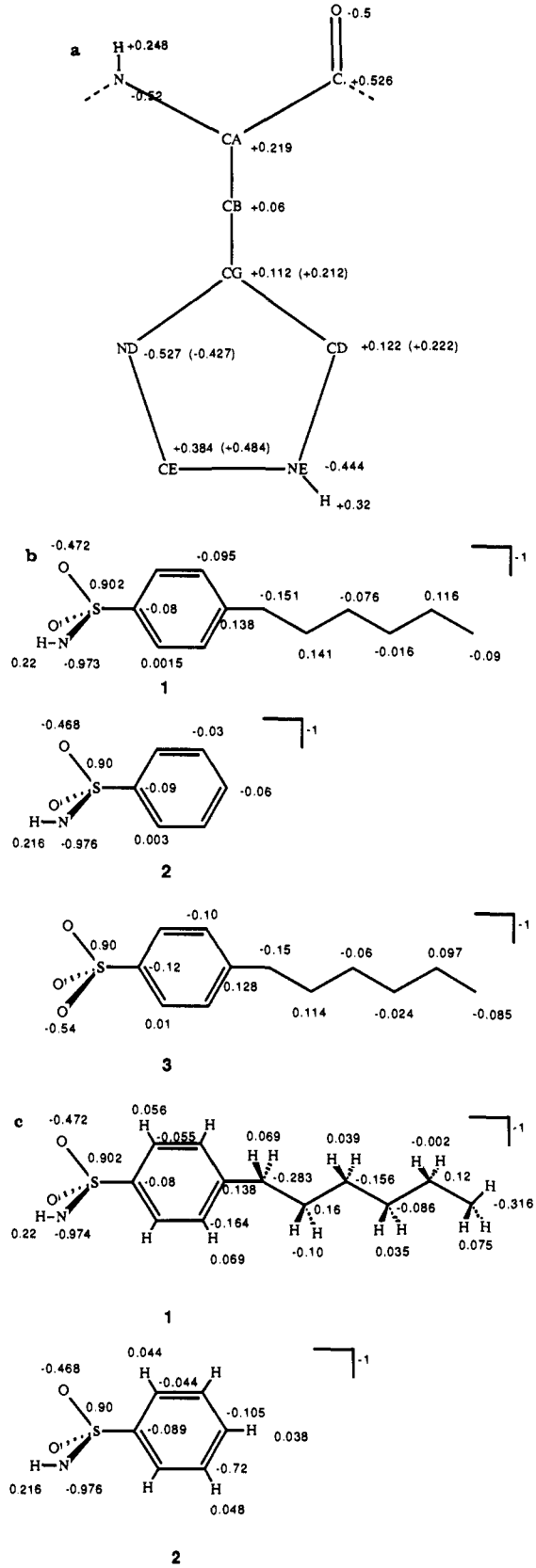

Figure 2. (a) Charges used for the modified AMBER HIE residue, (b) united-atom charges for **1**–**3**, and (c) the all-atom charges for **1** and **2**. The original AMBER united-atom charges[16a] for HIE are given with the modified charges in parentheses.

(16) (a) Weiner, S. J.; Kollman, P. A.; Case, D. A.; Singh, U. C.; Ghio, C.; Alagona, G.; Profeta, S.; Weiner, P. *J. Am. Chem. Soc.* **1984**, *106*, 765. (b) Weiner, S. J.; Kollman, P. A.; Nguyen, D. T.; Case, D. A. *J. Comput. Chem.* **1986**, *7*, 230.
(17) Hariharan, P. C.; Pople, J. A. *Chem. Phys. Lett.* **1972**, *66*, 217.
(18) Dewar, M. J. S.; Thiel, W. *J. Am. Chem. Soc.* **1977**, *99*, 4899, 4907.
(19) Singh, U. C.; Kollman, P. A. *J. Comput. Chem.* **1984**, *5*, 129.
(20) Collins, J. B.; Schleyer, P. v. R.; Binkley, J. S.; Pople, J. A. *J. Chem. Phys.* **1976**, *64*, 5142.
(21) Singh, U. C.; Weiner, P. K.; Caldwell, J. W.; Kollman, P. A. AMBER (UCSF), Version 3.0.
(22) Jorgensen, W. L.; Chandrasekhar, J.; Madura, J.; Impey, R. W.; Klein, M. L. *J. Chem. Phys.* **1983**, *79*, 926.
(23) Berendsen, H. J. C.; Potsma, J. P. M.; van Gunsteren, W. F.; DiNola, A. D.; Haak, J. R. *J. Phys. Chem.* **1984**, *81*, 3684.

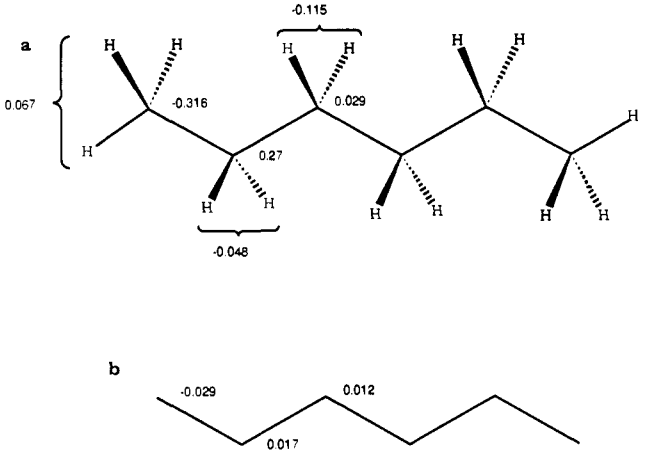

Figure 3. Charges used for the (a) all-atom and (b) united-atom representation of **4**.

shrink and no-shrink protocol with both the united-atom[16a] and the all-atom[16b] AMBER force fields, with any eye on determining which of these four possible approaches is best for the simulation of processes of this sort.

For the enzyme simulations the following protocol was followed: the coordinates supplied to us were first partially minimized (200 steps of minimization) to remove any bad contacts that were present. A cap of approximately 300 TIP3P waters with a radius of 22 Å centered on the zinc ion was placed over the active site. This cap was then restrained at the 22-Å boundary by a harmonic potential with a force constant of 0.5 kcal/Å. All residues 15 Å or more from the zinc ion were fixed, while the residues within 15 Å and the water molecules were allowed to move during the course of the MD run. The enzyme–substrate complex was then equilibrated at 300 K for 4 ps, which was subsequently followed by free energy simulations. The protocol that was used for these simulations is identical with that given above. The nonbonded pair list had a cutoff of 10.0 Å and was updated every 50 time steps. A constant dielectric of 1 was used throughout.

We found for the solution runs that these simulations suffered from a fair amount of hysteresis (i.e., $\Delta\Delta G_{sol}(\lambda=1\rightarrow0) \neq \Delta\Delta G_{sol}(\lambda=0\rightarrow1)$). We, therefore, decided to use the slow-growth method to evaluate the free energy for all four of the solution simulations.[8] This method has been previously shown to converge more rapidly than the window method, and we decided to see if it would also be the case here.[24] For these simulations we used identical conditions as described above, except that we ran these simulations over 40 ps in each direction using a 0.002-ps time step. We also used the final coordinate sets (λ = 1) from the window simulations to start these simulatioins because it offered us the advantage of starting with a more thoroughly equilibrated starting structure. SHAKE was used in order to allow us to make 0.002-ps time steps.[25] Thus, these simulations covered a total of 80 ps.

We have also done simulations converting hexane (**4**) to nothing in water in order to better compare our computed free energies to experimental free energies of solvation. The charges used for the hexane molecule were determined using 6-31G* ESP calculations.[19] For the united-atom case the charges were determined by restraining all of the hydrogen atoms to have a partial charge of 0.0, while the carbon atom charges were fit to best reproduce the quantum mechanically determined ESP potential.[19] The calculated charges are given in Figure 3. All other parameters used (bond, angle, torsion angle, and Lennard-Jones parameters) were taken from the standard AMBER united- and all-atom parameter sets.[16] The procedure followed was identical with that for the slow-growth runs described above except that the simulations were set up by first minimizing the hexane/water box to a rms gradient of less than 0.1 kcal/Å before 10 ps of equilibration at constant temperature (300 K) and pressure (1 atm). The free energies were determined over 50 ps of simulation in both the forward and reverse directions. All simulations used a 2-fs time step except for the all-atom shrink case where, because of problems with SHAKE, we used a time step of 1 fs.

In order to compare our results to experiment, we have made use of I_{50} (the concentration of inhibitor that decreases the velocity of catalysis to 50% of its uninhibited value) values. The I_{50} values have been shown to be of similar magnitude and highly correlated to K_I values.[4] Furthermore, the $\Delta\Delta G_{bind}$ values calculated from I_{50} and K_I data usually agree to within ±0.25 kcal/mol.[4] Thus, we have used I_{50}'s to determine our experimental $\Delta\Delta G_{bind}$ values. The I_{50} values we have used are 3.5 nM, 350 nM, and 4.9 μM for **1**–**3**, respectively. For **3** the I_{50} value given is that for benzenesulfonate and not the *p*-hexyl derivative. Thus, assuming that the hexyl substituent gives a constant contribution to the binding constants, we have compared our calculated results for **1** → **3** with the difference given by 350 nM and 4.9 μM.

Table II. Calculated ΔG_{sol}, ΔG_{bind}, and $\Delta\Delta G_{bind}$ for the Processes **1** → **2** (Ia–IVb) and **1** → **3** (V) (Experimental $\Delta\Delta G_{bind}$ Given for Comparison; All Values in Kilocalories per Mole)

run[a]	ΔG_{sol}	ΔG_{bind}	$\Delta\Delta G_{bind}$	$\Delta\Delta G_{bind}$ (expt)
		1 → 2		
Ia	4.67 ± 1.1	4.23 ± 0.75	−0.44 ± 1.33	
Ib	5.2 ± 0.22	4.23 ± 0.75	−0.97 ± 0.78	
IIa	0.03 ± 1.51[b]	4.99 ± 0.47	4.96 ± 1.58	
IIb	2.1 ± 1.16	4.99 ± 0.47	2.89 ± 1.25	
IIIa	3.02 ± 1.26	5.65 ± 0.15	2.63 ± 1.27	
IIIb	4.48 ± 0.96	5.65 ± 0.15	1.17 ± 0.97	
IVa(1)	−1.24 ± 1.02	1.21 ± 0.96	2.45 ± 1.4	
IVa(2)	1.56 ± 0.35	2.93 ± 1.06	1.37 ± 1.12	
IVa(3)	1.03 ± 0.22	3.17 ± 0.06	2.15 ± 0.23	
IVb	0.51 ± 1.2	3.17 ± 0.06	2.66 ± 1.20	2.73
		1 → 3		
V	7.73 ± 0.24	12.42 ± 0.35	4.69 ± 0.42	1.57 5.04[c]

[a] An a indicates that ΔG_{sol} and ΔG_{bind} were determined by the window method, while b indicates that ΔG_{sol} was determined by the slow-growth method and the ΔG_{bind} value used to determine $\Delta\Delta G_{bind}$ is the same as in (a). For the all-atom no-shrink case (IVa), we have carried out three sets of simulations (1–3). These correspond to simulation times of 32.8, 82, and 164 ps. [b] This is averaged over two sets of window runs, not one, as was the case for all other runs. [c] Corrected by using eq 6; see the text and Table III.

Results

The first simulation we carried out for the conversion of **1** to **2** used the united-atom shrink protocol. The results are given in Table II (Ia,b). The ΔG_{sol} calculated by the windowing method was 4.7 ± 1.1 kcal/mol, while it was 5.2 ± 0.22 kcal/mol for the slow-growth method. These results suggest that the *p*-hexylbenzene compound is much better solvated than the benzene one, which at first glance is counterintuitive. This issue will be further discussed in the following section. The computed value for ΔG_{bind} is 4.2 ± 0.75 kcal/mol, giving a final value for $\Delta\Delta G_{bind}$ of −0.44 ± 1.33 kcal/mol (windows) and −0.97 ± 0.78 kcal/mol (slow growth). This suggests that **2** is a better inhibitor than **1**. However, the experimental number of 2.73 kcal/mol favors **1**.

The next set of simulations used the united-atom no-shrink protocol (see Table II; IIa,b). In our initial test runs using this approach for the enzyme simulations, we found that the end point (λ = 0) the free energy increases rapidly because we are "turning off" the hexyl group parameters completely at this point. In order to mitigate this problem, we used the window method up to the next to last window (λ = 0.025) and from this point we used the slow-growth method up to a λ value of 6.0×10^{-5}. The appropriate window and slow-growth free energies were then pieced together. Note that the implicit assumption here is that the free energy obtained on going from $\lambda = 6.0 \times 10^{-5}$ to λ = 0 can be assumed to be negligible. We feel that this assumption is justified because of the very small $\Delta\lambda$ step involved. The ΔG_{sol} calculated in this way is 0.03 ± 1.51 kcal/mol. In the slow-growth simulations we again observed that the computed free energy increases rapidly at the end of the simulation. Thus, we only ran these simulations to the penultimate step ($\lambda = 5.0 \times 10^{-5}$). Our rationale for this is identical with that used when using the window method. The free energy computed in this way is 2.1 ± 1.16 kcal/mol, which has a smaller error bar range associated with it, but it is further away from the "experimental value" (see below). The computed ΔG_{bind} is 4.99 ± 0.47 kcal/mol, which yields us a final value of 4.96 ± 1.58 kcal/mol (windows) and 2.89 ± 1.25 kcal/mol (slow growth) for $\Delta\Delta G_{bind}$. The value for $\Delta\Delta G_{bind}$ computed with the window method is in fair agreement with experiment, while in

(24) Berendsen, H. J. C. In *Molecular Dynamics and Protein Structure*; Hermans, J., Ed.; Polycrystal Book Service: Western Springs, IL, 1985; p 18.
(25) van Gunsteren, W. F.; Berendsen, H. J. C. *Mol. Phys.* **1977**, *34*, 1311.

the case of the hybrid-window (ΔG_{bind}) and slow-growth (ΔG_{sol}) approach the agreement with experiment is excellent. Thus, while the individual numbers for ΔG_{bind} and ΔG_{sol} may be incorrect, the difference between them yields a value for $\Delta\Delta G_{bind}$ that is close agreement with the experimental result. This observation will be discussed further in the following section.

We next went on to test the all-atom shrink protocol (see Table II; IIIa,b). The computed ΔG_{sol} values for the window and slow-growth methods are 3.02 ± 1.26 and 4.48 ± 0.96 kcal/mol, respectively. The computed ΔG_{bind} is 5.65 ± 0.15 kcal/mol, and as in the other enzyme simulations the hysteresis is within acceptable limits. The calculated $\Delta\Delta G_{bind}$ values using the all-window (2.63 ± 1.27 kcal/mol) and hybrid (1.17 ± 0.97 kcal/mol) approaches are in good agreement with the experimental value, but in this case the hybrid approach does not fare quite as well as the all-window approach.

The final simulation in this series employed the all-atom no-shrink protocol (see Table II; IVa(1-3),b). For IVa(1-3) we report three sets of simulations: the first covers 32.8 ps, the second 82 ps, and the third 164 ps. In the first case the computed window ΔG_{sol} (−1.24 ± 1.02 kcal/mol) is negative, while the slow-growth method (IVb; 0.51 ± 1.2 kcal/mol) and the longer window runs (1.56 ± 0.35 and 1.03 ± 0.22 kcal/mol) are all positive. The value for ΔG_{bind} in this instance ranges from 1.21 ± 0.96 to 3.17 ± 0.06 kcal/mol (see Table II). When each of these are combined with their respective ΔG_{sol}'s, we obtain $\Delta\Delta G_{bind}$'s in the range of 1.37 ± 1.12 to 2.66 ± 1.20 kcal/mol, all of which are in reasonable accord with experiment. The hybrid approach using the best ΔG_{bind} (IVa(3)) also yields a $\Delta\Delta G_{bind}$ in good accord with experiment (2.66 ± 1.2 kcal/mol). We note that these simulations were also subject to a rapid change in the computed free energies at $\lambda = 0$. Hence, we used the same procedure as described in the united-atom no-shrink section (see above) to avoid this problem.

The conversion of **1** into **3** involves the mutation of the sulfonamide moiety into a sulfonate group. The results for this set of simulations is given in Table II (see V). We find from the solution simulations that the sulfonamide is predicted to be better solvated than the sulfonate by 7.7 ± 0.24 kcal/mol. No experimental data exist for this change, but we feel that the sign for this conversion is correct but the magnitude may be a bit large. For the enzyme simulations we find that the sulfonamide is better bound by 12.4 ± 0.35 kcal/mol. Combining these numbers, we get a prediction for the $\Delta\Delta G_{bind}$ of 4.7 ± 0.47 kcal/mol, which is much greater than the experimental value. However, there is a problem when we compare the apparent binding constant determined experimentally and the intrinsic binding constant we determine theoretically because of the pK_a difference between a sulfonate (2.55[26]) and a sulfonamide (9.95).

The binding of sulfonamides shows a strong pH dependence, which results in a bell-shaped curve for the log of the apparent association constant K_{app} vs pH. This observation is thought to be due to (1) the ionization equilibrium of the sulfonamide moiety, which accounts for the high-pH behavior, and (2) the ionization equilibrium of the enzyme, which accounts for the low-pH part of the curve. These data suggest two possible kinetic mechanisms for the binding of an inhibitor with CA[1]

$$E^+ + L^- \rightleftharpoons E^+ - L^- \quad (4)$$

$$E + L \rightleftharpoons E^+ - L^- \quad (5)$$

where E^+ is the zinc–water form of HCAII, E is the zinc–hydroxide form, L is the neutral, and L^- is the ionized form of the inhibitor. Mechanism 4 has the zinc–water form of the enzyme binding with the anionic form of the inhibitor, while reaction 5 has the zinc–hydroxide form of the enzyme binding to the neutral form of the inhibitor. Whether reaction 4 or 5 is the dominant pathway has been the subject of some controversy.[1]

Given that K_{app} is defined as [EL]/[E][L], the following expressions can be derived, for cases 4 and 5 above, that give the relationship between the observed binding constant (K_{app}) and the intrinsic affinity constant (K_I)[1]:

$$K_{app} = K_I' \frac{1}{\left(1 + \frac{K_a'}{[H^+]}\right)\left(1 + \frac{[H^+]}{K_a''}\right)} \quad (6)$$

$$K_{app} = K_I'' \frac{1}{\left(1 + \frac{[H^+]}{K_a'}\right)\left(1 + \frac{K_a''}{[H^+]}\right)} \quad (7)$$

$$K_a' = \frac{[E][H^+]}{[E^+]} \qquad K_a'' = \frac{[L^-][H^+]}{[L]}$$

These equations simply describe how the pH dependence of the various pH-sensitive groups affect the intrinsic binding constant to yield an apparent binding constant. Thus, we can take the observed apparent binding constants (I_{50}) and the K_a's for the enzyme (K_a' here) and inhibitor (K_a'' here) and determine the intrinsic K_I for both case 4 and 5. Our calculations address the issue of the difference in stability of the anions bound to the enzyme and in solution and, therefore, eq 6 is the appropriate relationship to use in order to determine the intrinsic or true binding constant. This value can then be directly compared to our calculated $\Delta\Delta G_{bind}$ since the pH dependence has been removed.

Table III. Evaluation of the Intrinsic K_I Using Equation 6[a]

	K_I (M^{-1}, kcal/mol)
1	3.57×10^9, −13.03
3	7.27×10^5, −7.99
$\Delta\Delta G_{bind}$	5.04 kcal/mol

[a] K_a' was assumed to be 1×10^{-7}, and the pH ([H^+]) is 7.4. K_{app} for **1** is 2.86×10^6 M^{-1}, and the K_{app} for **3** is assumed to be 2.04×10^5 M^{-1}. K_a'' values for **1** and **3** were taken to be 1.12×10^{-10} and 2.79×10^{-3}, respectively. [b] The $\Delta\Delta G_{bind}$ are given for **1** → **3**.

The results are given in Table III. The K_{app} values are taken directly from the experimental values discussed in Computational Procedure. For the enzyme ionization constant K_a' we used a value of 1×10^{-7} and we assumed the [H^+] to be 3.98×10^{-8} based on the pH (7.4) at which the experimental values were determined. The experimental ionization constants (K_a'') for the inhibitors were 1.12×10^{-10} and 3.16×10^6 for **1** and **3**, respectively. Taking the individual K_I' values determined from eq 6 for the binding of **1** and **3**, we get 5.04 kcal/mol for $\Delta\Delta G_{bind}$, which is in excellent agreement with our calculated value of 4.7 kcal/mol for **1** → **3**.

The quality of our results, for the mutation of **1** → **3**, supports the reasonableness of our charge model for the active site. We should note that the quoted experimental value is for the conversion of **2** → benzenesulfonate. It is our expectation that this value and the one for **1** → **3** should be similar. Note that the hysteresis observed in all of these calculations is rather small, suggesting that our simulation time scale is satisfactory for this electrostatics dominated conversion.

Discussion

As stated in the Introduction, the conversion of a hexyl group to nothing is a very ambitious undertaking given the large environmental reorganization that must take place in such a process. However, we feel it important to push our techniques to their limit in order to garner a deeper understanding of their capabilities and limitations. Simultaneously, this research has given us qualitative insight into the inhibition of HCAII. In what follows we will address the simulation issues and discuss the chemical insight this work has produced.

The determination of the free energy differences using the free energy perturbation method in conjunction with molecular dynamics can be subject to a fair amount of hysteresis (i.e., $\Delta G_{A\rightarrow B} \neq \Delta G_{B\rightarrow A}$). In order to reduce the amount of hysteresis observed, one has to be acutely aware of the relaxation time scale for the system under scrutiny. This is because the accuracy of a free

(26) Kortüm, G.; Vogel, W.; Andrusson, K. *Pure Appl. Chem.* **1961**, *1*, 187.

energy perturbation simulation is directly related to the adequacy of the sampling of phase space. Since the free energy is integrated over the phase space available to the system, the accuracy of the results strongly depends on how effective phase space is sampled by the simulation. If entropy is a strong contributor to the free energy, then it is even more important to have sampled phase space extensively. Thus, if the simulation is carried out over a time scale that is much greater than the relaxation time scale for the system, it can be expected that the observed hysteresis should be small (i.e., the simulation is reversible). If the simulation is run over a time scale similar to that for the relaxation process, we expect that the free energy determined in the reverse direction will not be identical with the forward direction. A pitfall occurs if the simulation is run over a shorter period of time than the relaxation process, because the determined free energies would appear to be very accurate (i.e., no hysteresis) when in fact they may be very inaccurate because of inadequate sampling of phase space. No firm guidelines are available to decide how long a simulation should be run to get converged results. The solution-phase simulations of 32.8 ps (windows) and 80 ps (slow growth) in general might be considered long enough to sufficiently sample phase space, but since we are dealing with a very conformationally flexible solute, they could potentially be too short. This is reflected in our observed hysteresis. For the enzyme simulations it can be argued that the time scale is too short (32.8 ps).

In order to address these issues, we have carried out free energy simulations of 32.8, 82, and 164 ps for the all-atom no-shrink cases (cases IVa(1–3), respectively). For the solution-phase simulations we see that there is a fair amount of variability in the calculated free energies (about a 2 kcal/mol range) but that the longer runs (IVa(2,3) and the 80-ps slow-growth run IVb) seem to be converging at a value of about 1 kcal/mol for the difference in the free energy of solvation of **1** and **2**. For the enzyme runs, the longer simulations are converging to a value around 3 kcal/mol, while the shorter run predicted a free energy of binding of 1.2 kcal/mol. How does this variability affect the relative free energies of binding? From our results it seems that there is not a large effect. The variability in the calculated $\Delta\Delta G_{bind}$ values is at the 1 kcal/mol level, with the short run being in as good agreement as the much longer simulations. Thus, as has been observed before,[8] the use of free energy cycles compensates for the fluctuation in free energies calculated from different simulation time scales.

The roughly conical active site of HCAII is divided into a hydrophilic half and a hydrophobic half. Thus, the inhibitors that we are studying here can take advantage of the active site dichotomy by interacting with the hydrophobic region of the active site. This is indeed what we observe for **1**. To start our enzyme simulations (i.e., **1** → **2**), we placed the inhibitor in the central region of the active site, and as we equilibrated, we found that the hexyl tail tended toward the hydrophobic portion of the active site. In general, we found that the enzyme simulations are subject to a smaller amount of hysteresis, whereas the solution runs are subject to much more (see Table II). The reason for this is now obvious: the hexyl tail from **1** interacts with the hydrophobic portion of the active site and restricts the conformational space available. In the solution simulations, the hexyl tails are fluxional and, therefore, it is unlikely that we have sampled all of the available conformational space during the course of a relatively short simulation. Thus, we would expect and indeed observe that the hysteresis in the solution simulations is greater than that in the enzyme runs.

From the data of Table II on **1** → **2** we observe that shrink protocol gives ΔG_{sol} values that are large and positive, in contrast to the no-shrink protocol, which gives free energies that are significantly smaller. Unfortunately, we do not have an experimental value for the ΔG_{sol} of **1** → **2** that we can use to assess the reliability of our results. In order to better compare to experiment we have carried out simulations on hexane (**4**) to nothing in order to determine which simulation protocol is giving us the best free energies. The results are given in Table IV. These results clearly indicate that only the no-shrink all-atom model is giving the most reliable free energies. The experimental value for the free energy of solvation of **4** is 2.55 kcal/mol,[27] and the calculated value using the all-atom no-shrink protocol is 2.77 ± 0.56 kcal/mol, which is in excellent agreement with experiment. We believe that the no-shrink all-atom protocol gives ΔG_{sol} values that are in resonable accord with experiment, and therefore, we can assume that the ΔG_{sol} for **1** → **2** is probably on the order of +1 kcal/mol. The shrink protocol tends to always give free energies that are large and positive, potentially because we are not using an approach that couples the coordinates with the perturbation parameter λ.[28]

Table IV. ΔG_{sol} Values (kcal/mol) for Conversion from Nothing to Hexane

run	ΔG_{sol}(calc)	ΔG_{sol}(expt)[a]
united-atom shrink	−4.10 ± 0.35	
united-atom no-shrink	−0.27 ± 0.16	
all-atom shrink	−3.66 ± 0.55	
all-atom no-shrink	2.77 ± 0.56	2.55

[a] See ref 26.

In several of the simulations we found that the calculated free energy rapidly increased when the hexyl tail was annihilated at λ = 0. Right before λ = 0 is reached the hexyl tail has finite Coulombic and Lennard-Jones parameters, which disappear when λ = 0 is reached. Thus, the potential that was restraining intermolecular interactions is removed, and rapid changes in the system are possible, which then results in the rapid nonphysical increase in the calculated free energies. This effect has also been seen by other groups.[8] In order to circumvent this problem, we have run our simulations until the penultimate step in λ, which in our simulations left a residual λ of 6.0×10^{-5}. This approach is justified in that it is expected that if small enough steps in λ could be taken to complete the simulation, the overall contribution to the total calculated free energy would be small.

The accurate representation of active site metal ions (a catalytic zinc ion in this case) with force field methods requires great care. From our work it is obvious that the treatment of a divalent ion as a +2.0 point charge causes a large perturbation in the region surrounding the point charge. The assignment of a +2.0 charge to zinc is based on purely formalistic considerations, and it is almost certain that the charge on the zinc ion should be significantly less than +2.0. Furthermore, the use of constraints,[10] while probably useful in cases where energy minimization is being used, can limit the conformational space of the system and, therefore, can alter computed free energies.

To improve this situation, we have devised the model detailed in Parametrization. This approach has solved the problem of retaining a reasonable active site structure in cases where the electrostatic energy dominates the perturbation (i.e., **1** → **3**), and it appears to give a reasonable free energy for the relative binding affinities.

The active site dichotomy suggests that in designing inhibitors for HCAII it is also advantageous to take into account the hydrophobic or hydrophilic portions of the active site. For example, in all of our simulations on **1** → **2** we find that the *p*-hexyl compound has a stronger interaction with the HCAII active site than does the phenyl compound due to the favorable hydrophobic interactions between **1** and the active site. In general, most of the effective HCAII inhibitors are hydrophobic in nature, and probably all, to some extent, take advantage of the favorable hydrophobic interactions that are possible in the active site.[4] Hydrophilic interactions (hydrogen bonds, etc.) between the R group of a sulfonamide and the active site of HCAII are likely to be important too, but because of the compounds we have chosen we are presently unable to address this issue. However, it is safe to say that hydrophilic interactions are more directional (i.e., hydrogen-bond formation) relative to hydrophobic interactions and that in order for latter to enhance binding affinity great care would have to be taken in the design of the compound.

(27) Ben-Naim, A.; Marcus, Y. *J. Chem. Phys.* **1984**, *81*, 2016.
(28) Rao, B. G.; Singh, U. C. *J. Am. Chem. Soc.* **1989**, *111*, 3125.

The simulations reported here have also provided us with structural insight into why sulfonamides are better inhibitors than are sulfonates. As mentioned in the Introduction (see Figure 1) the sulfonamide moiety forms two hydrogen bonds with Thr 199 in the HCAII active site. The first is between the sulfonamide hydrogen and the hydroxyl oxygen of Thr 199 and the second is between the main-chain NH hydrogen and the sulfonamide oxygen atom, which is not bound to the zinc ion. The other oxygen atom and the nitrogen atom are directly coordinated to the zinc ion present in the HCAII active site. Thus, all atoms that are part of the sulfonamide are involved in some sort of stabilizing interaction, be it via hydrogen bonds or electrostatic interactions with the zinc ion. In the sulfonate case only the main-chain NH and inhibitor oxygen hydrogen bond is possible. The other hydrogen bond is absent and is replaced with a repulsive O···O interaction between Thr 199 and the sulfonate inhibitor. We find from the end point structure for our simulation of **1** to **3** that the net result of this repulsive interaction is to force Thr 199 to rotate out of the conformation observed in the sulfonamide structures. This results in a diminishment of the repulsive interaction, but results in the breaking of the hydrogen bond between the hydroxyl hydrogen of Thr 199 and the carboxyl oxygens of Glu 106. Two of the sulfonate oxygens are symmetrically bound to the zinc ion, in contrast to the distant coordination of an oxygen atom and a tighter interaction with the nitrogen atom in the sulfonamide case. Thus, the sulfonate lacks one important hydrogen bond, which contributes to the poorer binding of sulfonates relative to sulfonamides. This is reminiscent to the situation in thermolysin where a 4.1 kcal/mol difference in binding between a phosphonate and a phosphoramidate inhibitor was traced directly to a hydrogen-bond interaction present in the latter, but not the former, inhibitor.[10] Thus, at least part of the difference in binding affinity of **3** relative to **1** is due to the loss of this hydrogen bond.

Conclusions

The free energy perturbation method has been successfully applied to the binding of sulfonamide and sulfonate inhibitors of HCAII. In order to carry out these simulations, we found that we had to develop a new approach for the incorporation of metal ions into force fields that include electrostatic interactions. We found that the metal ion charge has to be reduced, with the extra charge being placed on the associated ligands surrounding the metal ion. This approach has been validated by the fact that our computed relative free energies for conversion of **1** into **3** are in good agreement with experiment. Furthermore, the fact that our active site model is able to maintain the experimentally observed structure of the HCAII active site is further proof of its reasonableness.

We find that the hexyl tail simulations can be done most effectively with no-shrink methodologies, but a *general* solution for the simulation of conformational flexible molecules still has not been developed.[29] Regardless, our computed $\Delta\Delta G_{bind}$'s determined from the no-shrink protocol are in reasonable agreement with experiment, which can be attributed to cancellation of errors between the calculated ΔG_{sol} and ΔG_{bind} values. Furthermore, simulations done on hexane to nothing suggest that the all-atom no-shrink approach is preferable to all other employed here in that it is capable of determining ΔG_{sol} values that are in reasonable accord with experiment. Furthermore, the all-atom no-shrink model has performed considerably better than the other models and should be used whenever possible. However, we again note that the use of a thermodynamic cycle allows for fortuitous cancellations of errors between ΔG_{sol} and ΔG_{bind} values, which certainly enhances the usefulness of these techniques in areas like rational drug design. It is clear that the free energy perturbation method is capable of routinely being within ±2.0 kcal/mol of experiment.[8] Furthermore, it is clear that an error of ±1.0 kcal/mol is possible for electrostatically dominated processes like **1** to **3** here, but for van der Waals dominated processes, like **1** to **2**, the errors are larger due to conformational effects.[8]

The present simulations also clearly indicate that one of the major contributing factors to the lower binding affinity of sulfonates for HCAII is due to the disruption of a hydrogen-bond interaction between Thr 199 and the amide hydrogen from a sulfonamide. Other factors are likely to have an influence, but the one obvious structural difference in the binding of sulfonamides relative to sulfonates is this missing hydrogen bond.

Acknowledgment. We acknowledge research support from the NIH (Grant GM-29072). The facilities of the UCSF computer graphics laboratory supported by Grant RR-1081 are gratefully acknowledged as is the supercomputer time from the San Diego Supercomputer Center and from the Cornell National Supercomputer Center facility, both supported by the NSF and the latter also by New York State and IBM. We thank Dr. H. Schwam, Dr. S. R. Michelson, and J. M. Sondey for determining the I_{50} values for **1–3**. Finally, K.M.M. thanks Shashi Rao and Carol Fierke for many helpful discussions and R. Hoffmann for supplying us with some of his computer resources.

(29) Straatsma, T. P.; McCammon, J. A. *J. Chem. Phys.* **1989**, *90*, 3300.